Synthetic and Systems Biotechnology 10 (2025) 381–390

Contents lists available at ScienceDirect

Synthetic and Systems Biotechnology

journal homepage: www.keaipublishing.com/en/journals/synthetic-and-systems-biotechnology

Original Research Article

Metabolic engineering of *Glarea lozoyensis* for high-level production of pneumocandin B_0

Xinyi Zhang [a,b], Shu Cheng [a], Jing Yang [a], Li Lu [a], Zixin Deng [a,c], Guangkai Bian [b,*], Tiangang Liu [a,c,**]

[a] Key Laboratory of Combinatorial Biosynthesis and Drug Discovery, Ministry of Education and School of Pharmaceutical Sciences, Wuhan University, 430072, Wuhan, China

[b] Center of Materials Synthetic Biology, CAS Key Laboratory of Quantitative Engineering Biology, Shenzhen Institute of Synthetic Biology, Shenzhen Institutes of Advanced Technology, Chinese Academy of Sciences, 518055, Shenzhen, China

[c] State Key Laboratory of Microbial Metabolism, Joint International Research Laboratory of Metabolic & Developmental Sciences, and School of Life Sciences and Biotechnology, Shanghai Jiao Tong University, 200030, Shanghai, China

ARTICLE INFO

Keywords:
Antifungal drug
Echinocandins
Pneumocandin B_0
Multi-omics
Systems metabolic engineering

ABSTRACT

Pneumocandin B_0 (PB_0) is a lipohexapeptide synthesized by *Glarea lozoyensis* and serves as the precursor for the widely used antifungal drug caspofungin acetate (Cancidas®). However, the low titer of PB_0 results in fermentation and purification costs during caspofungin production, limiting its widespread clinical application. Here, we engineered an efficient PB_0-producing strain of *G. lozoyensis* by systems metabolic engineering strategies, including multi-omics analysis and multilevel metabolic engineering. We overexpressed four rate-limiting enzymes: thioesterase GLHYD, two cytochrome P450s GLP450s, and chorismate synthase GLCS; knocked out two competing pathways responsible for producing 6-methylsalicylic acid and pyranidine E; and overexpressed the global transcriptional activator GLHYP. As a result, the PB_0 titer increased by 108.7 % to 2.63 g/L at the shake-flask level through combinatorial strategies. Our study provides valuable insights into achieving high-level production of PB_0 and offers general guidance for developing efficient fungal cell factories to produce polyketide synthase-non-ribosomal peptide synthetase hybrid metabolites.

1. Introduction

Invasive fungal diseases (IFDs) represent a notable global healthcare burden, accounting for over 300 million severe cases and 1.5 million deaths annually [1]. In October 2022, the World Health Organization published a landmark report identifying the first-ever list of fungal "priority pathogens", highlighting the urgent need to address fungal infections [2]. Over the past four decades, only two novel classes of antifungal drugs—echinocandins and triterpenoids (ibrexafungerp)—have been developed as inhibitors of β-1,3-D-glucan synthesis in fungal cell walls [3]. Due to their high efficacy and low toxicity, echinocandins have rapidly become first-line therapies for treating IFDs [4]. Caspofungin, the first licensed echinocandin, is semi-synthesized from the lipohexapeptide pneumocandin B_0 (PB_0) produced by the filamentous fungus *Glarea lozoyensis*. The global market for caspofungin is expected to reach USD 560.3 million by 2026, positioning it as the top-selling echinocandin [5]. However, high fermentation and purification costs, driven by low PB_0 titer, make caspofungin expensive and unaffordable for many patients. Thus, enhancing the production of PB_0 is a pressing necessity.

Strain breeding and optimization of fermentation processes have been widely employed to increase PB_0 titers. In one study, mutagenesis was employed to develop a high-yield strain, Q1, which achieved a PB_0 titer of 1.87 g/L [6]. Additionally, the introduction of 1.0 g/L sodium dodecyl sulfate on day 13 of the extractive batch fermentation increased the PB_0 titer by 37.6 % [7]. In 2013, An's group identified the pneumocandin biosynthetic gene cluster, establishing a foundation for the targeted metabolic engineering of high-yield PB_0-producing strains [8]. Following this discovery, the basic steps involved in PB_0 biosynthesis were gradually elucidated (Fig. 1A) [9–12], and efforts were made to

* Corresponding author.
** Corresponding author. Key Laboratory of Combinatorial Biosynthesis and Drug Discovery, Ministry of Education and School of Pharmaceutical Sciences, Wuhan University, 430072, Wuhan, China.
E-mail addresses: gk.bian@siat.ac.cn (G. Bian), liutg@whu.edu.cn (T. Liu).

https://doi.org/10.1016/j.synbio.2024.12.008
Received 16 October 2024; Received in revised form 2 December 2024; Accepted 20 December 2024
Available online 24 December 2024

manipulate the pneumocandin biosynthetic gene cluster to increase PB_0 production. The disruption of *GLoxy4* gene eliminated the by-product pneumocandin A_0 [4]. The CRISPR/Cas9 gene editing technology was used to replace *gloF* with *ap-htyE*, leading to the elimination of pneumocandin C_0 [13]. However, systematic metabolic engineering studies on *G. lozoyensis* that integrate multi-omics analyses and multilevel strategies—such as substrate supply optimization, competitive metabolism elimination, and transcriptional regulation—are still scarce.

Systems metabolic engineering strategies are increasingly used to increase the titers of important secondary metabolites, thanks to a deeper understanding of biosynthetic pathways and their regulation in microorganisms [14–16]. These approaches typically begin with systematic omics analysis and then optimize strains using multilevel metabolic engineering techniques [17–19], such as rate-limiting gene overexpression [20], operon restructuring and promoter engineering [21], cofactor supply engineering and recycling [22], and elimination of competing pathways [23]. In our previous work, we combined metabolomic and proteomic analyses with *in vitro* reconstitution to guide synthetic pathway editing [17]. Various valuable chemicals, such as fatty acids, their derivatives, and terpenoids, were efficiently produced using *Escherichia coli* and *Saccharomyces cerevisiae* [24–26]. Moreover, multilevel metabolic engineering strategies have been successfully applied to *Streptomyces roseosporus*, leading to an increase in daptomycin production to 113 mg/L in shake-flask fermentation, representing a 565 % improvement over the starting strain [23]. Therefore, systems metabolic engineering is an effective strategy to enhance the production of important secondary metabolites.

In this study, we employed systems metabolic engineering strategies

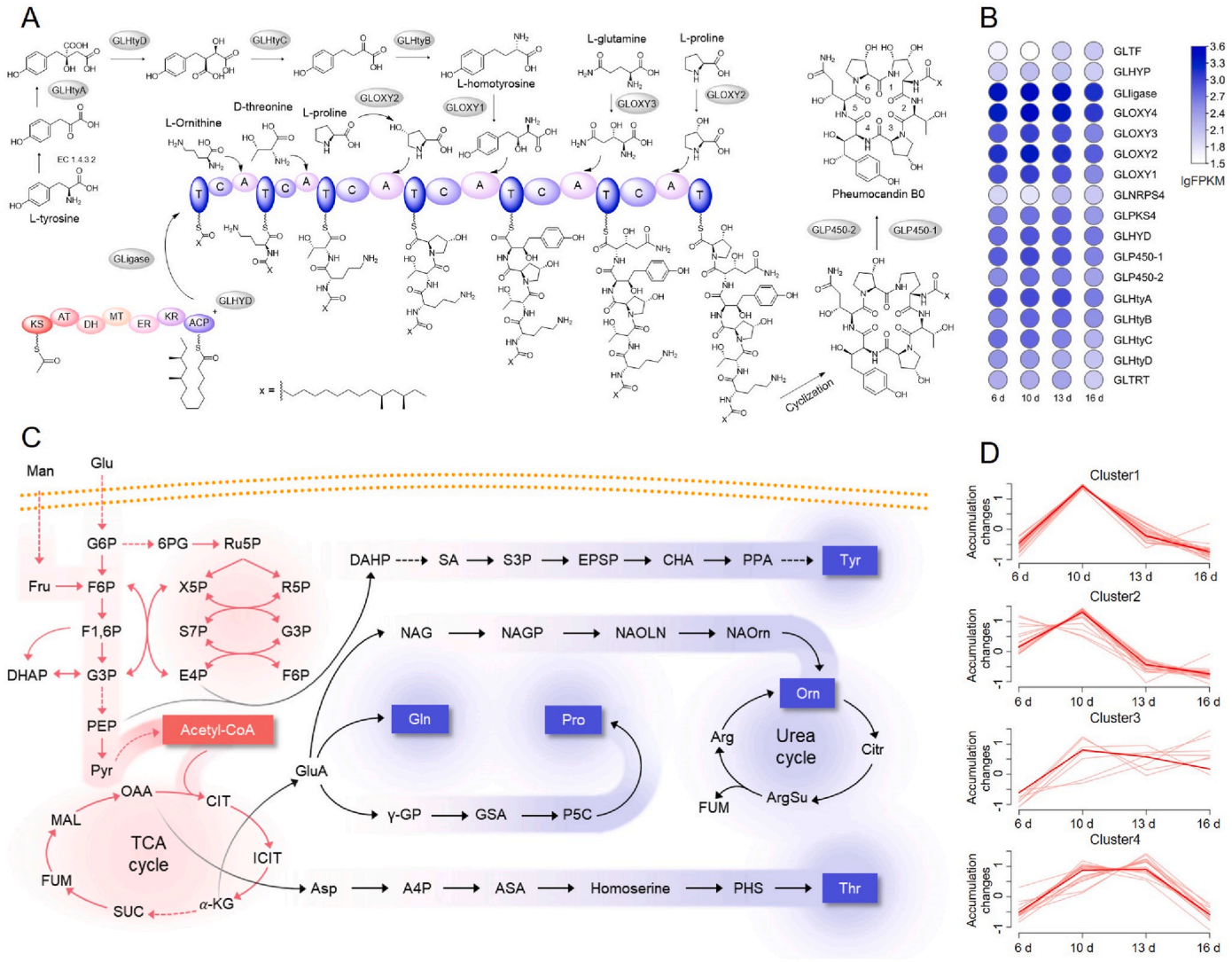

Fig. 1. Multi-omics analysis of PB_0-producing *G. lozoyensis*. (A) Schematic representation of PB_0 biosynthesis. (B) Heatmap of the expression levels of functional genes within the PB_0 cluster. (C) Schematic of the essential pathways in *G. lozoyensis* responsible for converting glucose and mannitol to PB_0. (D) Time-course analysis of the accumulation of major metabolites in key PB_0 biosynthesis pathways. The peak intensity of each metabolite was standardized based on the dry weight of the cell debris. The level of each metabolite on fermentation day 6 was defined as "1", and the metabolite levels on days 10, 13, and 16 were expressed as their fold changes on day 6. The intensities of intracellular metabolites were evaluated in triplicate. Man, mannitol; Glu, glucose; Fru, fructose; G6P, glucose-6-phosphate; F6P, fructose-6-phosphate; F1,6P, fructose-1,6-bisphosphate; G3P, glyceraldehyde-3-phosphate; DHAP, dihydroxyacetone phosphate; PEP, phosphoenolpyruvate; Pyr, pyruvate; 6-PG, gluconate-6-phosphate; Ru5P, ribulose-5-phosphate; X5P, xylulose-5-phosphate; R5P, ribose-5-phosphate; S7P, sedoheptulose-7-phosphate; E4P, erythrose 4-phosphate; DAHP, 3-deoxy-arabino-heptulosonate-7-phosphate; SA, shikimate; CHA, chorismate; PPA, prephenate; NAG, N-acetylglutamate; NAGP, N-acetylglutamyl-phosphate; NAOLN, N-Acetyl-5-oxo-L-norvaline; NAOrn, N-acetyl-ornithine; Citr, citruline; FUM, fumarate; ArgSu, argininosuccinic acid; GluA, glutamate; γ-GP, γ-glutamyl phosphate; GSA, glutamate-5-semialdehyde; P5C, 1-pyrroline-5-carboxylate; Asp, aspartic acid; A4P, l-4-aspartyl-phosphate; ASA, L-aspartate-4-semialdehyde; PHS, homoserine phosphate; OAA, oxaloacetate; CIT, citrate; ICIT, isocitrate; α-KG, α-ketoglutaric acid; SUC, succinate; MAL, malate.

based on multi-omics analysis to increase the titer of PB_0 in *G. lozoyensis*. Initially, we used transcriptomic and metabolomic data to identify and optimize the rate-limiting steps and competing metabolites involved in PB_0 biosynthesis. Following this, we optimized the transcriptional regulation of PB_0 biosynthesis. By combining these effective high-yield methods, we developed a high-yield strain that significantly increased PB_0 titer by 108.7 %, reaching 2.63 g/L in shake-flask cultures. Overall, this study presents a comprehensive strategy to increase the titer of echinocandins for industrial production, aiming to reduce production costs and alleviate the financial burden associated with treating fungal infections.

2. Materials and methods

2.1. Strains, media, and growth conditions

All strains used or engineered in this study are listed in Table S1. The original strain of *G. lozoyensis* used in this study (Z00) was obtained from ATCC 74030 through atmospheric and room-temperature plasma (ARTP) mutagenesis. *G. lozoyensis* was cultivated in 30 mL of seed medium for 3 days at 25 °C and 220 rpm. 5 mL of seed culture (V0) was centrifuged at a speed of 3200 *g* for a duration of 15 min. Then the supernatant (V1) was collected to calculate the packed mycelial volume (PMV), defined mathematically as $PMV = (V0 - V1)/V0 \times 100\%$. Thereafter, the PMV was adjusted to 15 %. A 50 mL volume of the fermentation medium was then inoculated with 5 mL of the adjusted seed culture and cultivated for 13 days at 25 °C for PB_0 production assays.

The medium was prepared according to Qin's method with slight modifications [6]. The seed medium contained 40 g/L of glucose, 20 g/L of cottonseed powder, 1.5 g/L of KH_2PO_4, and 10 mL/L of trace element solution. The initial pH was adjusted to 6.0. The trace elements solution contained 1.0 g/L of $MnSO_4{\cdot}H_2O$, 1.0 g/L of $FeSO_4{\cdot}7H_2O$, 0.1 g/L of $ZnSO_4{\cdot}7H_2O$, 0.025 g/L of $CuCl_2{\cdot}2H_2O$, 0.01 g/L of $CaCl_2{\cdot}2H_2O$, 0.056 g/L of H_3BO_3, and 0.0003 g/L of $(NH_4)\ Mo_7O_{24}{\cdot}4H_2O$. The fermentation medium contained 20 g/L of glucose, 80 g/L of mannitol, 20 g/L of cottonseed power, 2 g/L of K_2HPO_4. The initial pH was 6.5.

2.2. RNA extraction, RNA-Seq and transcriptome analysis

For transcriptome analysis, *G. lozoyensis* was cultured for 16 days in 50 mL of fermentation medium. We took samples on the exponential (6 and 10 days) and stationary (13 and 16 days) growth phases. Thereafter, mycelium was collected, instantaneously frozen in liquid N_2, and stored at −80 °C in preparation for RNA extraction. Total RNA was isolated using a RNeasy Plant Mini Kit (Qiagen) following the supplier's instructions. The RNA samples were treated with RNase-free DNase I (Takara Bio) for 15 min to eliminate genomic DNA. RNA sequencing was conducted by Nevogene (Beijing, China), and the results were used to analyze the expression profiles of *G. lozoyensis* genes. Thereafter, corresponding expression levels were obtained through the calculation of fragments per kilobase of transcript per million mapped reads (FPKM). The results were visualized with TBtools based on the Euclidean distance calculation [27].

2.3. Metabolite extraction and analysis

To conduct a comprehensive analysis of omics data, fermentation broths were extracted and analyzed on days 6, 10, 13, and 16. The cells were extracted as previously described with slight modifications [28]. In brief, a cold (−30 °C) 100 % (v/v) methanol solution was promptly added to quench 5 mL of fermentation broth. After centrifugation at 5000*g* and 4 °C for 10 min, the mycelia was dropped into liquid N_2. A solvent mixture of methanol, acetonitrile, and H_2O in the ratio of 2:2:1 (v/v/v), pre-cooled to −30 °C, was employed to extract metabolites. The mycelium were transferred to a pre-cooled centrifuge tube (10 mL), followed by the sequential addition of glass beads (2 mm) and 2 mL of extraction solvent. The extraction process executed through three cycles of mechanical disruption (a cycle lasted for 60 s, followed by a 10 s break) using a vortex mixer. Then the supernatant was collected via centrifugation at 12,000 *g* and 4 °C for 20 min and freeze-dried. The powders were then prepared using 50 % (v/v) methanol, and employed for metabolite analysis. The mycelia debris was dried at 65 °C until the constant weight was reached. The determination of intracellular metabolites, metabolite identification, and statistical analyses were performed as described by Fu et al. [28] The time-course analysis was generated using R software (v.4.2.2) package "Mfuzz" through Hiplot Pro (https://hiplot.com.cn/) [29].

2.4. Construction of overexpression plasmid

All plasmids used in this study are listed in Table S2. All primers used are listed in Table S3. The DNA fragments of *GLtf*, *GLhyd*, *GLhyp*, *GLp450-1*, *GLp450-2,* and *GLcs* were amplified from the genomic DNA of *G. lozoyensis* (RefSeq: GCF_000409485.1) using the respective primer pairs. These fragments were cloned into vector pGB114 [30] at the restriction sites of *Hind*III/*Mre*I, and the resulting plasmids were designated as pYX33, pYX34, pYX35, pYX36, pYX37, pYX40, and pYX41, respectively. To construct the combinatorial overexpression plasmid, the expression cassettes of P*glgpdA*-*GLhyd*-T*glgpdA*, P*glgpdA*-*GLp450-1*-T*glgpdA*, P*glgpdA*-*GLp450-2*-T*glgpdA,* and P*glgpdA*-*GLcs*-T*glgpdA* were amplified from the corresponding plasmids using the respective primer pairs and cloned into pYX41 sequentially at the restriction sites of *Xba*I, *Spe*I, *Not*I, and *Pac*I, resulting in plasmids pYX45, pYX46, pYX47, pYX48, pYX49, pYX50, and pYX51, respectively. All the overexpression plasmids were introduced into *G. lozoyensis* through protoplast transformation. The accession numbers of genes are listed in Table S4.

2.5. Construction of knockout plasmid

To achieve high-efficiency gene knockout, we used the CRISPR/Cas9 system. Specific genomic RNA (sgRNA) sequences targeting *GLhyp*, *GLpyrE,* and *GL6-MA* were obtained using the open-source tool http://www.biotool.com (Table S5) [31]. For *GLhyp* knockout, the sgRNA scaffold fragment was amplified from pSC249 using the primer pair *GLhyp*-N20-F/U6ter-R. 5S rRNA of *G. lozoyensis* and its upstream sequence were amplified from *G. lozoyensis* genome using a primer pair of 5S–F and *GLhyp*-N20-R. The two fragments were thereafter assembled into a sgRNA expression cassette via overlap extension polymerase chain reaction (OE-PCR)using a primer pair of 5S–F and U6ter-R. The *Bam*HI/*Not*I-digested sgRNA expression cassette targeting *GLhyp* was inserted into pSC251 (*Bam*HI/*Not*I-digested) [32] to generate pYX42, which was transformed into *G. lozoyensis* to disrupt *GLhyp*. This approach was used to construct pYX38, pYX39, and pYX44.

2.6. Transformation of G. lozoyensis

G. lozoyensis was transformed as described by Dong et al. with some modifications [33]. 200 μL of protoplast suspension were gently mixed with 50 μL of precooled polyethylene glycol (PEG) transformation solution (40 % PEG6000, 100 mM $CaCl_2$, 50 mM Tris-HCl, pH 7.5) and 5 μg of DNA fragment in a pre-chilled 15 mL centrifuge tube. After a 20 min incubation on ice, 2 mL of the PEG transformation solution was thoroughly mixed in and then incubated statically at 25 °C for 5 min. Finally, 4 mL of sorbitol solution (1.2 M sorbitol, 10 mM $CaCl_2$, and 10 mM Tris-HCl, pH 7.5) was added. The mixture was spread on PDA plates containing 1 M sorbitol and 150 μg/mL geneticin or 200 μg/mL hygromycin B at 25 °C. The recombinant strains were identified, following the extraction of genomic DNA and PCR verification.

2.7. Quantitation of pneumocandin B_0

The concentration of PB_0 was detected by high-performance liquid chromatography (HPLC). Mixed 3 mL of broth with 5 mL of ethanol, subjected to sonication for 30 min. The mixture was centrifuged at 3200 *g* for 15 min, and the supernatant was analyzed using an ODS C18 HPLC column (4.6 × 250 mm, 5 μm, Agela, Tianjin). For HPLC, a mixture of 57 % water and 43 % acetonitrile (v/v) was used as the mobile phase at a flow rate of 1.0 mL/min and eluted for 20 min. The process was monitored at 220 nm.

3. Results and discussion

3.1. Multi-omics analysis of PB_0-producing *G. lozoyensis*

We conducted multi-omics analyses of *G. lozoyensis* to accurately identify the rate-limiting steps for targeted engineering. The gene expression profile and density map clarified the overall transcriptional level of the strain (Fig. S1). RNA-sequencing analysis revealed that fragments per kilobase of transcript per million mapped (FPKM) values for most genes ranged from 1 to 100, with a mode around 20. A cluster-level transcriptome analysis (Fig. 1B) revealed significant disparities in the expression levels of functional genes. The expression levels of oxygenase genes (*GLoxy1*, *GLoxy2*, *GLoxy3*, and *GLoxy4*) and acyltransferase gene (*GLligase*) were notably high, with FPKM values exceeding 1000 by the 10th day, and in some cases surpassing 2000. Conversely, the expression levels of the other genes were lower, indicating possible rate-limiting steps, necessitating a comprehensive analysis alongside other omics data.

Hence, we evaluated the intracellular metabolite profiles during shake-flask fermentation of *G. lozoyensis*. We compared the dynamic changes in major metabolites, including metabolites from central carbon metabolism pathways, such as glycolysis, the pentose phosphate pathway, the citric acid cycle, and amino acids that serve as substrates for PB_0 biosynthesis (Fig. 1C). Time-course analysis indicated that the metabolites could be categorized into four distinct clusters (Fig. 1D).

Notably, within cluster 3, seven metabolites showed persistent accumulation, representing potential rate-limiting steps (Fig. S2). Among these, asparagine was identified as a primary metabolite not directly involved in PB_0 biosynthesis, while 4-phospho-L-aspartate (PAsp), *cis*-aconitate (CA), and 5-enolpyruvylshikimate-3-phosphate (EPSP) were key primary metabolites associated with PB_0 biosynthesis. The remaining three metabolites in this cluster were pneumocandin F (PF), pneumocandin B_2 (PB_2), and the cyclic scaffold (CycS) of PB_0. By integrating the aforementioned omics data, we systematically identified the bottlenecks in PB_0 biosynthesis in *G. lozoyensis* and performed targeted engineering to address these limitations.

3.2. Identification and overexpression of rate-limiting enzymes to improve PB_0 production

Promoters play a crucial role in metabolic engineering and synthetic biology by activating silent biosynthetic gene clusters and optimizing biosynthetic pathways of important natural products [21]. To identify suitable promoters for the genetic modification of *G. lozoyensis*, we characterized a series of promoters prior to engineering. β-Glucuronidase was used as the readout to determine the strength of the promoters ranked as follows: P*glgpdA* > P*amyB* > P*gpdA* > P*hlyA* > P*glaA* > P*alcA* > P*trpC* > P*enoA* > P*oliC* > P*agdA* (Fig. S3). Based on these results, the glyceraldehyde-3-phosphate dehydrogenase promoter of *G. lozoyensis* (P*glgpdA*) was selected as the preferred promoter for genetic modifications.

Overexpression of rate-limiting steps is a common strategy to improve the titers of important secondary metabolites [20,34]. Results from an association analysis of metabolite time-course and gene expression differences revealed key rate-limiting steps involved in the release of intermediates, redox processes, and substrate synthesis during PB_0 production. Initially, we focused on the secondary metabolic pathways involved in PB_0 biosynthesis. As previously mentioned, the metabolites in cluster 3 of the time-course analysis could be the rate-limiting steps (Fig. 1D), including the intermediate metabolites PF and PB_2 in the biosynthesis of PB_0 (Fig. S2). Two cytochrome P450 enzymes (GLP450-1 and GLP450-2) in the PB_0 cluster are responsible for converting PF and PB_2 into PB_0 by introducing hydroxyl groups on the L-homotyrosine residue and dihydroxylating L-ornithine, respectively (Fig. 2A). Insufficient activity of these two CYP450 enzymes may lead to the accumulation of PF and PB_2. The heatmap of expression level revealed that the expression levels of these two CYP450s were indeed lower than that of the other functional genes within the PB_0 cluster (Fig. 2B). Moreover, *GLligase* exhibited the highest expression level among the functional genes during the exponential growth (days 6 and 10) and early stationary (day 13) phases. For lipoinitiation in pneumocandin biosynthesis, the interaction between type II thioesterase GLHYD and acyl AMP-ligase GLligase is crucial (Fig. 2C) [9]. However, the expression level of *GLhyd* was significantly lower than that of *GLligase* (Fig. 2B), which may restrict the flow of GLligase-catalyzed reactions. Consequently, we speculate that *GLhyd*, *GLp450-1,* and *GLp450-2* are rate-limiting genes in PB_0 biosynthesis. To address this, we overexpressed these genes by randomly inserting one copy of each gene into the genome, constructing three engineered strains: Z11 (*GLhyd*), Z12 (*GLp450-1*), and Z13 (*GLp450-2*). In subsequent shake-flask fermentations, all mutant strains (Z11, Z12, and Z13) produced higher PB_0 titers than the original strain.

Notably, the PB_0 titer in Z11 increased to 1.62 g/L, representing a 28.6 % increase compared to that of the original strain (Fig. 2D). These results indicate that type II thioesterase GLHYD plays an important role in supplying the side chain (10, 12-dimethylmyristoyl), which significantly contributes to the production of lipopeptide. This finding aligns with the previous studies and highlights the essential role of type II thioesterases in the biosynthesis of polyketide synthase (PKS) and non-ribosomal peptide synthetase (NRPS) products [35]. Moreover, type II thioesterases often serve as rate-limiting steps in biosynthetic processes. For instance, maduramicin titer increased by 30 % to 7.16 g/L in shake-flask fermentation following the overexpression of type II thioesterase MadTE [34].

Subsequently, we focused on modifying key amino acids, particularly in the biosynthesis of 3-hydroxy homotyrosine (7). Metabolomic data revealed a significant decrease in the accumulation of 4-(4-hydroxyphenyl)-2-oxobutanoic acid (5) compared to the upstream metabolite 3-(4-hydroxy-benzyl)-malic acid (4) during the biosynthesis of 7 (Fig. 3A). Simultaneously, the heatmap of expression level indicated lower expression of the isopropyl malate dehydrogenase gene (*GLhtyC*), which is responsible for converting 4 to 5 within the gene cluster (Fig. 3B). To address this rate-limiting step, we overexpressed *GLhtyC* under the control of the P*glgpdA* promoter through random insertions, generating the mutant strain Z14 (*GLhtyC*). Contrary to our expectations, Z14 produced less PB_0 than the initial strain (Fig. 3D). One possible explanation for this is that the low expression of the downstream transaminase gene (*GLhtyB*) may also represent a rate-limiting step. Consequently, even with *GLhtyC* overexpressed, the subsequent reactions remained restricted, hindering significant improvements in PB_0 production.

Finally, we optimized the primary metabolic pathways relevant to PB_0 biosynthesis. Primary metabolic processes directly influence the synthesis of secondary metabolites, particularly NRPS, which utilize amino acids as central substrates. For example, the overexpression of key genes in the shikimate pathway to boost tyrosine supply can increase the yield of glycopeptide antibiotics [36]. Therefore, we analyzed the primary metabolic pathways related to PB_0 biosynthesis, particularly those involved in key amino acids synthesis, using multi-omics data. The results showed a significant accumulation of EPSP in cluster 3, with a remarkable 197-fold increase from day 6 to day 16 (Fig. S2). Meanwhile,

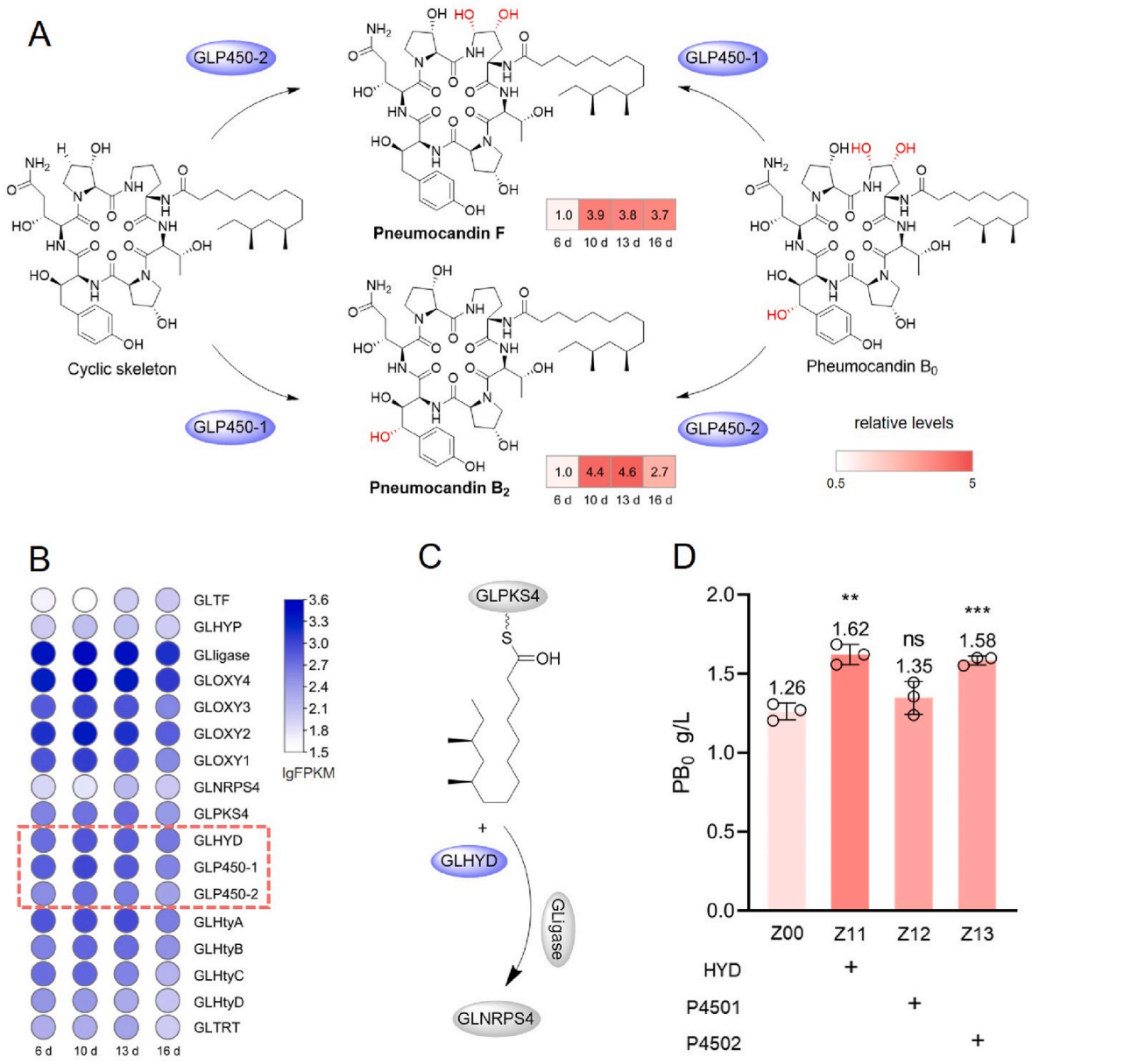

Fig. 2. Overexpression of rate-limiting enzymes in gene clusters enhances PB_0 production. (A) Schematic diagram of the biosynthesis and relative accumulation of the intermediate metabolites, PF and PB_2. (B) Heatmap showing the expression levels of functional genes within the PB_0 cluster. (C) Schematic diagram of the function of type II thioesterase GLHYD. (D) Flask cultivation results of the mutant strains. Data are presented as the mean ± SD (n = 3). Strain Z00 was used as the control. Statistical analysis was performed using a two-tailed Student's *t*-test (***$P < 0.001$, **$P < 0.01$, ns, $P \geq 0.05$).

the heatmap of expression level revealed a gradual decrease in the expression level of chorismate synthase GLCS (GLAREA_10520, GCA_000409485.1) over time, which is responsible for converting EPSP to chorismate. Additionally, the downstream metabolites, chorismate and prephenate, were not detected (Fig. 3C). Given the importance of this pathway in the synthesis of tyrosine, a precursor amino acid for the fourth module, we overexpressed the chorismate synthase gene (*GLcs*) via random insertion to generate the mutant strain Z15 (*GLcs*). PB_0 production by Z15 increased by 11.7 % compared to that of the parent strain, achieving a shake-flask titer of 1.53 g/L (Fig. 3D).

This increase indicates that low expression of *GLcs* limits PB_0 biosynthesis. However, the increase was less pronounced compared to the overexpression of *GLhyd*. This may be due to the pivotal role of chorismate in primary metabolism, which serves as a precursor for essential metabolites such as tyrosine, phenylalanine, and tryptophan. Consequently, the metabolic flux was scattered, and overexpression of a single *GLcs* copy was insufficient to significantly enhance PB_0 production. The analysis of metabolites from Z15 confirmed this hypothesis. The result indicates that *GLcs* overexpression led to a notable reduction in the excessive accumulation of EPSP. However, the accumulation of EPSP on day 13 remained approximately 21 times higher than that on day 6 (Fig. 4), while chorismate and prephenate remained undetected. This suggests that the catalytic efficiency of GLCS is still insufficient, indicating potential for further optimization. This process of identifying and engineering *GLcs* highlights the importance of targeted metabolic engineering guided by multi-omics data.

3.3. Eliminating competing metabolic pathways enhances substrate availability

Adequate substrate availability is a prerequisite for metabolite overproduction [37]. Knocking out unnecessary competitive pathways

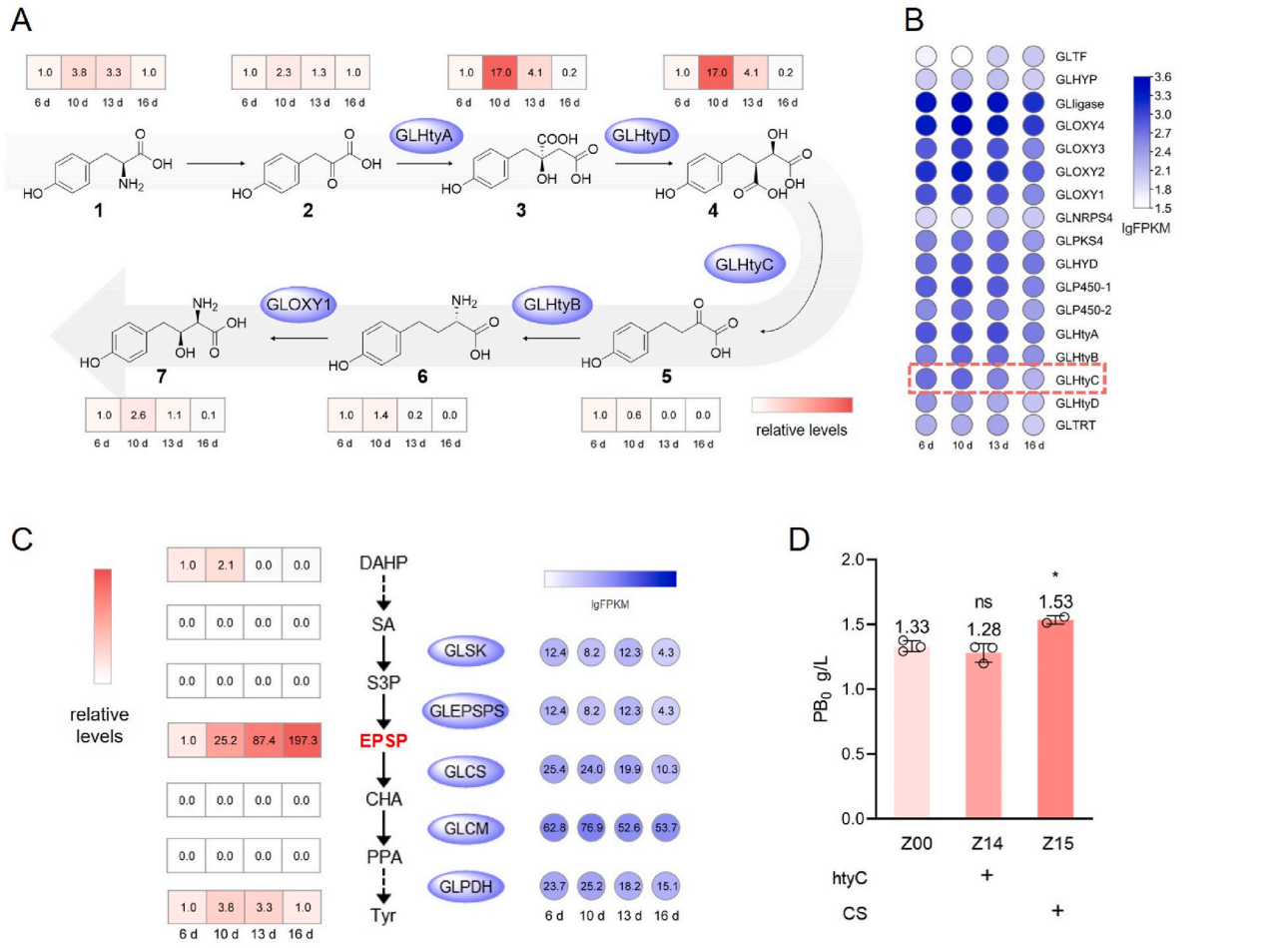

Fig. 3. Identification and overexpression of rate-limiting steps in the synthesis and modification of amino acid substrates. (A) Schematic diagram of the biosynthesis of 3-hydroxy-L-homotyrosine and the relative accumulation levels of the intermediates. 1, L-tyrosine; 2, 4-hydroxy-phenyl-pyruvate; 3, 2-(4-hydroxy-benzyl)-malate; 4, 3-(4-hydroxy-benzyl)-malate; 5, 4-(4-hydroxyphenyl)-2-oxobutanoic acid; 6, L-homotyrosine; 7, 3-hydroxy-L-homotyrosine. (B) Heatmap showing the expression levels of functional genes within PB_0 cluster. (C) Schematic illustration of tyrosine biosynthesis, relative accumulation levels of intermediates (pink), and expression levels of related enzymes (blue). (D) Flask cultivation results of the mutant strains. Data are presented as the mean ± SD (n = 3). Strain Z00 was used as the control. Statistical analysis was performed using a two-tailed Student's *t*-test (*$P < 0.05$, ns, $P \geq 0.05$).

Fig. 4. Effects of the overexpression of *GLcs* on EPSP and its related metabolites. (A) Metabolites produced by the original strain (Z00). (B) Metabolites produced by the mutant strain Z15 (*GLcs*). The level of each metabolite on day 6 of fermentation was defined as "1", and the metabolite levels on days 10, 13, and 16 were expressed as their fold changes on day 6. The accumulation of metabolites was evaluated in triplicate.

is an effective strategy to increase substrate availability and redirect metabolic flux toward target products. Analysis of the *G. lozoyensis* genome (RefSeq: GCF_000409485.1) using antiSMASH [38] identified two gene clusters that are 100 % similar to those responsible for the biosynthesis of 6-methylsalicylic acid (6-MA) and pyranidine E (pyrE) (Fig. S4). Notably, 6-MA is a polyketide, while pyrE is a hybrid of polyketides and non-ribosomal peptides, both of which compete for the acetyl-CoA substrate with PB_0. The metabolite time-course analysis and gene expression level (lgFPKM) confirmed the active transcription of both gene clusters and the detectable presence of their corresponding metabolites, with 6-MA accumulation continuously increasing over time (Fig. 5A and B). To improve PB_0 production, we knocked out the core genes in the pyrE (GLPKS3-NRPS, GCF_000409485.1) and 6-MA (GLPKS2, GCF_000409485.1) clusters, generating mutant strains Z16 (Δ*GLpyrE*) and Z17 (Δ*GL6-ma*), respectively (Fig. 5C). Shake-flask fermentation results revealed that both mutant strains produced higher PB_0 titers than the initial strain, with Z17 achieving a 35.0 % increase and reaching a final titer of 1.66 g/L (Fig. 5D).

The findings shown in Fig. 5 confirm that the biosynthesis of 6-MA and pyrE competes for the acetyl-CoA substrate and the insufficient availability of the acetyl-CoA substrate for PB_0 synthesis. Moreover, the accumulation of 6-MA was more apparent over time; therefore, the increase in PB_0 production by Z17 was more significant following the knockout of *GL6-ma*. Previous studies have emphasized the crucial role of acetyl-CoA availability in the synthesis of PKS and PKS-NRPS hybrid natural products [39]. Similar approaches, such as simultaneously increasing substrate levels and enhancing substrate utilization through the overexpression of related genes, have proven effective in achieving high yields of daptomycin [23].

3.4. Engineering of transcriptional regulators in PB_0 biosynthesis

Engineering transcription regulators is a direct and effective strategy to enhance the production of secondary metabolites [40]. There was a hypothesized transcriptional factor GLTF (GLAREA_10050, GCA_000409485.1) within the gene cluster [8], whose expression was lower than that of other functional genes (Fig. 6A). Consequently, we overexpressed *GLtf* and constructed the mutant strain Z20 (*GLtf*). However, PB_0 production of Z20 (*GLtf*) was significantly reduced (Fig. 6B). Recent studies suggest that GLTF specifically regulates GLOXY2 rather than serving as a global regulator of PB_0 biosynthesis [41]. Therefore, overexpression of *GLtf* may disrupt the balance of metabolic flux, ultimately leading to decreased PB_0 production.

Subsequently, we knocked out *GLhyp* and simultaneously overexpressed it through random insertion to engineer cluster-situated regulatory gene. This led to the construction of novel engineered strains Z18 (*GLhyp*) and Z19 (Δ*GLhyp*). Shake-flask fermentation of Z18 showed a significant increase in PB_0 titer, reaching 1.93 g/L, representing a 47.3 % improvement over the parent strain. In contrast, Z19 exhibited a significant decrease in PB_0 titer (Fig. 6C). These results align with recent findings, as a global positive regulator, *GLhyp* plays a crucial role in PB_0 biosynthesis [41]. Even in engineered strains, overexpression of *GLhyp* significantly enhances PB_0 titer. Moreover, this result is similar to the modification results of other NRPS products, such as the modifications of transcriptional regulatory gene of plinamycin, which increased its yield by 2.5 times when combined with an increase in the gene cluster copy [42].

3.5. Construction of a high-yield cell factory for PB_0 production using combinatorial metabolic engineering

Combinatorial metabolic engineering is an efficient strategy to optimize the biosynthesis of target metabolites [43]. In previous sections, we described a series of effective methods for increasing PB_0 production. These methods include the overexpression of rate-limiting enzymes such as GLHYD, GLp450-1, GLp450-2, and GLCS; the elimination of competitive metabolites (including 6-MA and pyrE); and the engineering of transcriptional activators such as GLHYP. We systematically combined these methods to maximize the beneficial effects.

Initially, we combined the overexpression of multiple rate-limiting enzymes and a transcriptional activator and designed a series of plasmids that sequentially combined overexpression of *GLhyd*, *GLp450-1*, *GLp450-2*, *GLcs*, and *GLhyp*, with one copy of each gene inserted. These plasmids were randomly integrated into the genome of *G. lozoyensis* to generate new strains, Z22-Z29. All engineered strains exhibited enhanced PB_0 production (Fig. 7A). Notably, strain Z26 (*GLhyp*:*GLcs*:*GLp450-2*) exhibited a substantial increase in PB_0 production, which reached a titer of 2.54 g/L in shake-flask culture, representing a

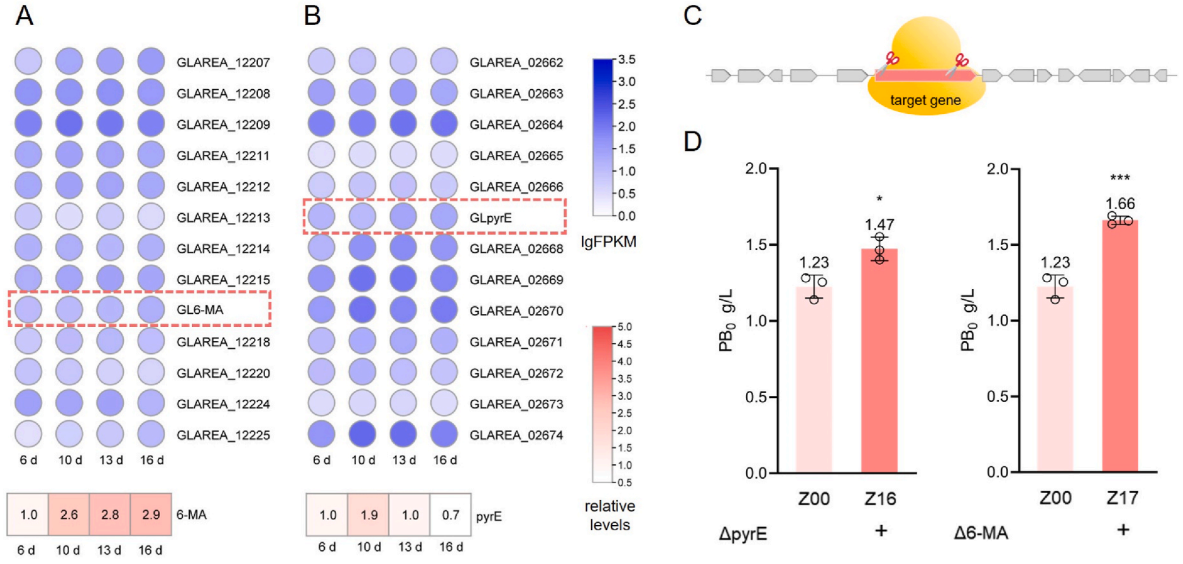

Fig. 5. Identification and elimination of competing metabolic pathways to enhance PB_0 production. (A) Accumulation level of the polyketide, 6-methylsalicylic acid (6-MA) (pink) and transcription of the 6-MA gene cluster (blue). (B) The accumulation level of pyranidine E (pyrE) (pink) and transcription of genes within the pyrE cluster (blue). (C) Schematic representation of target gene knockout using the CRISPR/Cas9 system. The core genes in the 6-MA and pyrE biosynthetic gene clusters were knocked out. (D) Shake-flask fermentation of the mutant strains. Data are presented as the mean ± SD (n = 3). Strain Z00 was used as the control. Statistical analysis was performed using a two-tailed Student's *t*-test (***$P < 0.001$, *$P < 0.05$).

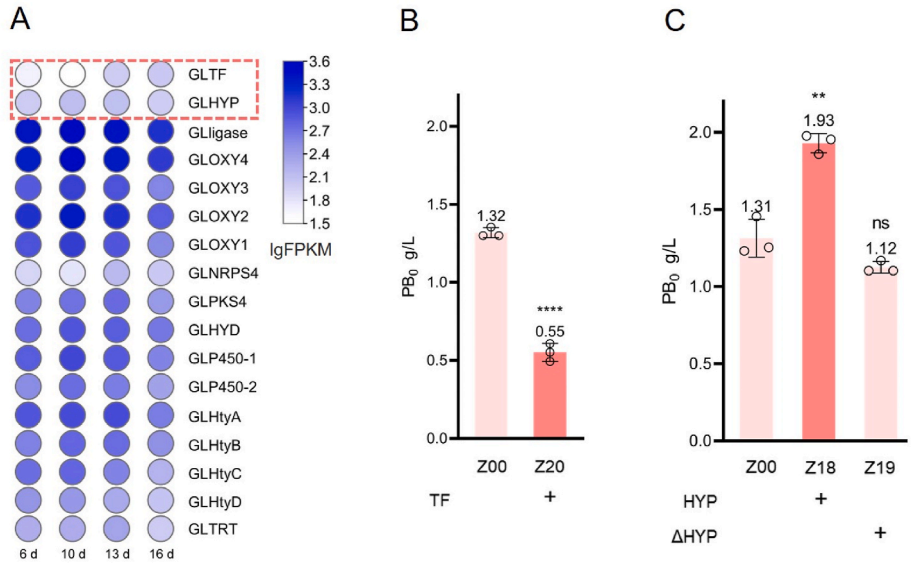

Fig. 6. Engineered cluster-situated regulatory genes increase PB_0 production. (A) Heatmap showing expression levels of functional genes within the PB_0 cluster. (B) Flask fermentation results of the mutant strain, Z20. (C) Flask fermentation results of the mutant strains, Z18 and Z19. Data are presented as the mean ± SD (n = 3). Strain Z00 was used as the control. Statistical analysis was performed using a two-tailed Student's *t*-test (****$P < 0.0001$, **$P < 0.01$, ns, $P \geq 0.05$).

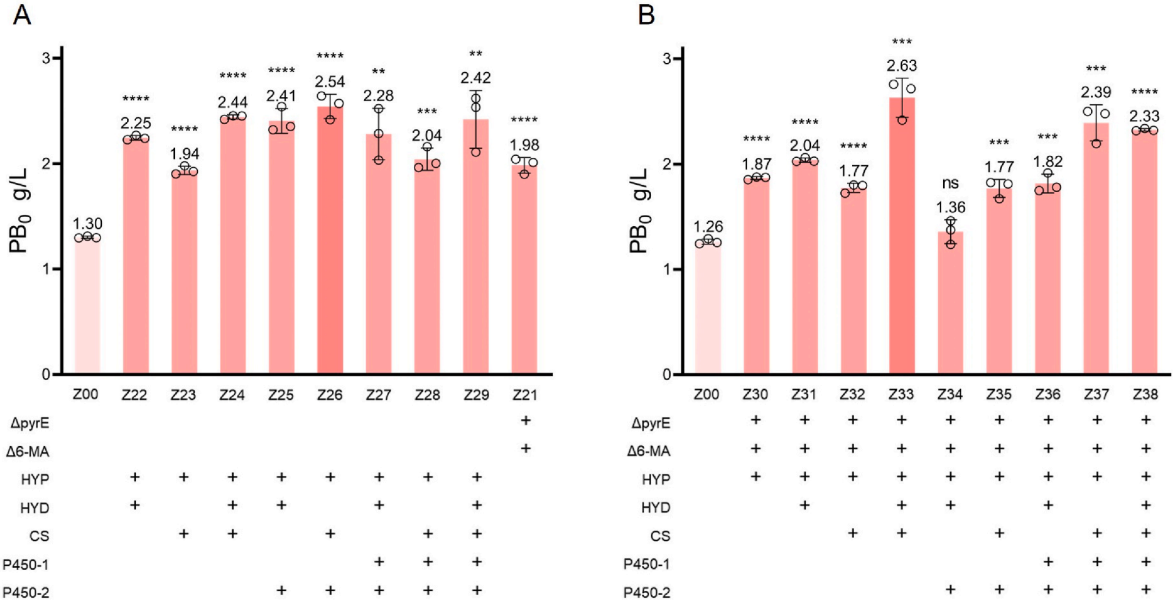

Fig. 7. PB_0 production in shake-flask fermentation of mutants using combinatorial metabolic engineering. (A) Mutants constructed by combining overexpression (Z22-Z29) and knockout methods (Z21). (B) Mutant strains constructed by combining overexpression approaches in mutant Z21 (Z30-Z38). Data are presented as the mean ± SD (n = 3). Strain Z00 was used as the control. Statistical analysis was performed using a two-tailed Student's *t*-test (****$P < 0.0001$, ***$P < 0.001$, **$P < 0.01$, ns, $P \geq 0.05$).

remarkable 95.4 % increase compared to the parent strain. However, the results were more intricate and varied than those observed with single gene overexpression, as the increase in yield was not directly proportional to the number of overexpressed genes. This complexity likely arises from the random insertion of target genes, which can create imbalances in metabolic flux.

Moreover, we constructed a double knockout mutant, Z21 (Δ*GL6-ma*Δ*GLpyrE*), using the CRISPR/Cas9 system to investigate the potential synergistic effect of deleting two competing metabolites of PB_0 biosynthesis. PB_0 production was further increased to 1.98 g/L at shake-flask level compared to the individual knockout of each single metabolite (Fig. 7A). Building on the success of these combinations, we attempted to further increase PB_0 titer by combining overexpression approaches in mutant Z21. As a result, mutant strain Z33 (*GLhyp*:*GLhyd*:*GLcs*, Δ*GL6-ma*Δ*GLpyrE*) exhibited the highest increase, with an impressive 108.7 % increase compared to the original strain, achieving a final production titer of 2.63 g/L in shake-flask fermentation. In this strain, the knockout of *GLpyrE* and *GL6-ma*, coupled with the overexpression of *GLcs* in primary metabolism, increased substrate supply and availability. Meanwhile the overexpression of *GLhyd* and the engineering of transcriptional activators enhanced the biosynthetic efficiency of the PB_0 cluster and accelerated substrate utilization. This strategy significantly increased the efficiency of PB_0 biosynthesis, similar to increasing productivity in industrial production lines by improving the availability of upstream

raw materials and the throughput of downstream product pipeline. However, the results were more intricate and varied than anticipated, similar to previous combinatorial overexpression strategies, with some mutants showing minimal improvements in PB_0 titer. Surprisingly, Z34 (*GLhyp*:*GLhyd*:*GLp450-2*, Δ*GL6-ma*Δ*GLpyrE*) produced lower PB_0 titer than Z21 (Fig. 7B). This unexpected result may stem from the random integration of target genes and discrepancies between different biosynthetic steps [44].

Overall, a more efficient cell factory with a higher PB_0 titer was constructed using systems metabolic engineering. These results demonstrate the effectiveness of systems metabolic engineering strategies in developing industrially competitive fungal strains with increased production capacity. The integrated multi-omics analysis provides a comprehensive understanding of the metabolic network associated with PB_0 biosynthesis, which is crucial for targeted metabolic engineering of productive strains. This strategy can also be used to optimize the production of other high-value natural products [45]. Previous studies have shown significant enhancement in L-valine production by systems metabolic engineering that relies on in silico simulation and transcriptome analysis [46].

Although combinatorial strategies can maximize the beneficial effects of various approaches, determining the optimal copy number of rate-limiting genes during the overexpression is crucial to enhance natural product production [47]. For example, a mutant strain overexpressing two copies of *mgcE* exhibited a 1.32-fold higher titer of mangicol J compared to that with a single copy [32]. Furthermore, there are further avenues for optimization in this strain, such as enhancing acetyl-CoA supply, overexpressing gene clusters, and cofactor engineering. For example, the overexpression of genes encoding antibiotic transporters can reduce end-product toxic effects and feedback inhibition [48]. The yield of PKS-NRPS hybrid bleomycin increased by 9.59 times in a strain containing six copies of the gene cluster [49]. Therefore, there remains substantial potential for further improvements, which will be the focus of our next study.

4. Conclusions

This study demonstrates the effective application of systems metabolic engineering strategies, based on multi-omics studies, to enhance PB_0 production by *G. lozoyensis*. By simultaneously overexpressing three rate-limiting enzymes and a transcriptional activator, while knocking out two competitive metabolic pathways, we significantly increased PB_0 titer to 2.63 g/L by 108.7 % in shake-flask cultures. However, there remains ample scope for further improvements in other areas, such as optimizing gene copy numbers and engineering cofactors. In summary, our findings offer important insights into efficient production of echinocandin antifungal agents, with reduced purification costs. Moreover, this research provides a valuable reference to overproduce structurally similar natural products and proposes a general strategy to develop high-yield industrial fungal strains.

CRediT authorship contribution statement

Xinyi Zhang: Writing – original draft, Visualization, Validation, Methodology, Investigation, Formal analysis, Conceptualization. **Shu Cheng:** Methodology, Formal analysis. **Jing Yang:** Validation, Methodology. **Li Lu:** Methodology, Formal analysis. **Zixin Deng:** Supervision, Resources. **Guangkai Bian:** Writing – review & editing, Supervision, Resources, Project administration, Funding acquisition, Conceptualization. **Tiangang Liu:** Writing – review & editing, Supervision, Resources, Project administration, Funding acquisition, Conceptualization.

Declaration of competing interest

The authors declare the following financial interests/personal relationships which may be considered as potential competing interests: One patent application based on the results in this study have been filed by Shenzhen Institute of Advanced Technology, Chinese Academy of Sciences.

Zixin Deng and Tiangang Liu are Founding Editor and Editorial Board Member for Synthetic and Systems Biotechnology, respectively. And they were not involved in the editorial review or the decision to publish this article.

Acknowledgements

This work was funded by the National Key R&D Program of China (2021YFC2102600), the National Natural Science Foundation of China (32370060 and 32070063), and the Shenzhen Science and Technology Program (JCYJ20241202124932044).

Appendix A. Supplementary data

Supplementary data to this article can be found online at https://doi.org/10.1016/j.synbio.2024.12.008.

References

[1] Li P, Tedersoo L, Crowther TW, Wang B, Shi Y, Kuang L, et al. Global diversity and biogeography of potential phytopathogenic fungi in a changing world. Nat Commun 2023;14:6482. https://doi.org/10.1038/s41467-023-42142-4.
[2] WHO fungal priority pathogens list to guide research, development and public health action. https://www.who.int/publications-detail-redirect/9789240060241 (accessed May 7, 2023).
[3] Hu X, Yang P, Chai C, Liu J, Sun H, Wu Y, et al. Structural and mechanistic insights into fungal β-1,3-glucan synthase FKS1. Nature 2023;616:190–8. https://doi.org/10.1038/s41586-023-05856-5.
[4] Chen L, Yue Q, Li Y, Niu X, Xiang M, Wang W, et al. Engineering of *Glarea lozoyensis* for exclusive production of the pneumocandin B_0 precursor of the antifungal drug caspofungin acetate. Appl Environ Microbiol 2015;81:1550–8. https://doi.org/10.1128/aem.03256-14.
[5] Deshmukh SK, Sridhar KR, Badalyan SM. Fungal biotechnology prospects and avenues. first ed. Boca Raton: CRC Press; 2022. https://doi.org/10.1201/9781003248316.
[6] Qin T, Song P, Wang X, Ji X, Ren L, Huang H. Protoplast mutant selection of *Glarea Lozoyensis* and statistical optimization of medium for pneumocandin B_0 yield-up. Biosci Biotechnol Biochem 2016;80:2241–6. https://doi.org/10.1080/09168451.2016.1196575.
[7] Yuan K, Huang B, Qin T, Song P, Zhang K, Ji X, et al. Effect of SDS on release of intracellular pneumocandin B_0 in extractive batch fermentation of *Glarea lozoyensis*. Appl Microbiol Biotechnol 2019;103:6061–9. https://doi.org/10.1007/s00253-019-09920-x.
[8] Chen L, Yue Q, Zhang X, Xiang M, Wang C, Li S, et al. Genomics-driven discovery of the pneumocandin biosynthetic gene cluster in the fungus *Glarea lozoyensis*. BMC Genom 2013;14:339. https://doi.org/10.1186/1471-2164-14-339.
[9] Chen L, Li Y, Yue Q, Loksztejn A, Yokoyama K, Felix EA, et al. Engineering of new pneumocandin side-chain analogues from *Glarea lozoyensis* by mutasynthesis and evaluation of their antifungal activity. ACS Chem Biol 2016;11:2724–33. https://doi.org/10.1021/acschembio.6b00604.
[10] Jiang W, Cacho RA, Chiou G, Garg NK, Tang Y, Walsh CT. EcdGHK are three tailoring iron oxygenases for amino acid building blocks of the echinocandin scaffold. J Am Chem Soc 2013;135:4457–66. https://doi.org/10.1021/ja312572v.
[11] Li Y, Chen L, Yue Q, Liu X, An Z, Bills GF. Genetic manipulation of the pneumocandin biosynthetic pathway for generation of analogues and evaluation of their antifungal activity. ACS Chem Biol 2015;10:1702–10. https://doi.org/10.1021/acschembio.5b00013.
[12] Petersen L, Olewinski R, Salmon P, Connors N. Novel proline hydroxylase activities in the pneumocandin-producing fungus *Glarea lozoyensis* responsible for the formation of trans 3- and trans 4-hydroxyproline. Appl Microbiol Biotechnol 2003;62:263–7. https://doi.org/10.1007/s00253-003-1264-0.
[13] Wei T-Y, Wu Y-J, Xie Q-P, Tang J-W, Yu Z-T, Yang S-B, et al. CRISPR/Cas9-based genome editing in the filamentous fungus *Glarea lozoyensis* and its application in manipulating gloF. ACS Synth Biol 2020;9:1968–77. https://doi.org/10.1021/acssynbio.9b00491.
[14] Ajikumar PK, Xiao W-H, Tyo KEJ, Wang Y, Simeon F, Leonard E, et al. Isoprenoid pathway optimization for taxol precursor overproduction in *Escherichia coli*. Science 2010;330:70–4. https://doi.org/10.1126/science.1191652.
[15] Amos GCA, Awakawa T, Tuttle RN, Letzel A-C, Kim MC, Kudo Y, et al. Comparative transcriptomics as a guide to natural product discovery and biosynthetic gene cluster functionality. Proc Natl Acad Sci U S A 2017;114:E11121–30. https://doi.org/10.1073/pnas.1714381115.
[16] Choi KR, Jang WD, Yang D, Cho JS, Park D, Lee SY. Systems metabolic engineering strategies: integrating systems and synthetic biology with metabolic engineering. Trends Biotechnol 2019;37:817–37. https://doi.org/10.1016/j.tibtech.2019.01.003.

[17] Bian G, Deng Z, Liu T. Strategies for terpenoid overproduction and new terpenoid discovery. Curr Opin Biotechnol 2017;48:234–41. https://doi.org/10.1016/j.copbio.2017.07.002.
[18] Tan G-Y, Zhu F, Deng Z, Liu T. In vitro reconstitution guide for targeted synthetic metabolism of chemicals, nutraceuticals and drug precursors. Synth Syst Biotechnol 2016;1:25–33. https://doi.org/10.1016/j.synbio.2016.02.003.
[19] Mo Q, Song W, Xue Z, Yuan J. Multi-level engineering of *Saccharomyces cerevisiae* for the synthesis and accumulation of retinal. Green Chem 2022;24:8259–63. https://doi.org/10.1039/D2GC03073J.
[20] Shang Y, Zhang P, Wei W, Li J, Ye B-C. Metabolic engineering for the high-yield production of polydatin in *Yarrowia lipolytica*. Bioresour Technol 2023;381:129129. https://doi.org/10.1016/j.biortech.2023.129129.
[21] Chen J, Zhang R, Zhang G, Liu Z, Jiang H, Mao X. Heterologous expression of the plant-derived astaxanthin biosynthesis pathway in *Yarrowia lipolytica* for glycosylated astaxanthin production. J Agric Food Chem 2023;71:2943–51. https://doi.org/10.1021/acs.jafc.2c08153.
[22] Chen R, Gao J, Yu W, Chen X, Zhai X, Chen Y, et al. Engineering cofactor supply and recycling to drive phenolic acid biosynthesis in yeast. Nat Chem Biol 2022;18:520–9. https://doi.org/10.1038/s41589-022-01014-6.
[23] Lyu Z-Y, Bu Q-T, Fang J-L, Zhu C-Y, Xu W-F, Ma L, et al. Improving the yield and quality of daptomycin in *Streptomyces roseosporus* by multilevel metabolic engineering. Front Microbiol 2022;13:872397. https://doi.org/10.3389/fmicb.2022.872397.
[24] Ma T, Shi B, Ye Z, Li X, Liu M, Chen Y, et al. Lipid engineering combined with systematic metabolic engineering of *Saccharomyces cerevisiae* for high-yield production of lycopene. Metab Eng 2019;52:134–42. https://doi.org/10.1016/j.ymben.2018.11.009.
[25] Zhu F, Zhong X, Hu M, Lu L, Deng Z, Liu T. In vitro reconstitution of mevalonate pathway and targeted engineering of farnesene overproduction in *Escherichia coli*. Biotechnol Bioeng 2014;111:1396–405. https://doi.org/10.1002/bit.25198.
[26] Liu Q, Zhang G, Su L, Liu P, Jia S, Wang Q, et al. Reprogramming the metabolism of oleaginous yeast for sustainably biosynthesizing the anticarcinogen precursor germacrene A. Green Chem 2023;25:7988–97. https://doi.org/10.1039/D3GC01661G.
[27] Chen C, Chen H, Zhang Y, Thomas HR, Frank MH, He Y, et al. TBtools: an integrative toolkit developed for interactive analyses of big biological data. Mol Plant 2020;13:1194–202. https://doi.org/10.1016/j.molp.2020.06.009.
[28] Fu S, An Z, Wu L, Xiang Z, Deng Z, Liu R, et al. Evaluation and optimization of analytical procedure and sample preparation for polar *Streptomyces albus* J1074 metabolome profiling. Synth Syst Biotechnol 2022;7:949–57. https://doi.org/10.1016/j.synbio.2022.05.004.
[29] Kumar L, Mfuzz E Futschik M. A software package for soft clustering of microarray data. Bioinformation 2007;2:5–7.
[30] Bian G, Han Y, Hou A, Yuan Y, Liu X, Deng Z, et al. Releasing the potential power of terpene synthases by a robust precursor supply platform. Metab Eng 2017;42:1–8. https://doi.org/10.1016/j.ymben.2017.04.006.
[31] Xie S, Shen B, Zhang C, Huang X, Zhang Y. sgRNAcas9: a software package for designing CRISPR sgRNA and evaluating potential off-target cleavage sites. PLoS One 2014;9:e100448. https://doi.org/10.1371/journal.pone.0100448.
[32] Yuan Y, Cheng S, Bian G, Yan P, Ma Z, Dai W, et al. Efficient exploration of terpenoid biosynthetic gene clusters in filamentous fungi. Nat Catal 2022;5:277–87. https://doi.org/10.1038/s41929-022-00762-x.
[33] Dong Y, Zhang L, Zhang W, Cao J, Wei Y, Song P, et al. Glyap1 regulates pneumocandin B_0 synthesis by controlling the intracellular redox balance in *Glarea lozoyensis*. Appl Microbiol Biotechnol 2021;105:6707–18. https://doi.org/10.1007/s00253-021-11522-5.
[34] Liu R, Fang F, An Z, Huang R, Wang Y, Sun X, et al. Genomics-driven discovery of the biosynthetic gene cluster of maduramicin and its overproduction in *Actinomadura* sp. J1-007. J Ind Microbiol Biotechnol 2020;47:275–85. https://doi.org/10.1007/s10295-019-02256-5.
[35] Geyer K, Hartmann S, Singh RR, Erb TJ. Multiple functions of the type II thioesterase associated with the phoslactomycin polyketide synthase. Biochemistry 2022;61:2662–71. https://doi.org/10.1021/acs.biochem.2c00234.
[36] Thykaer J, Nielsen J, Wohlleben W, Weber T, Gutknecht M, Lantz AE, et al. Increased glycopeptide production after overexpression of shikimate pathway genes being part of the balhimycin biosynthetic gene cluster. Metab Eng 2010;12:455–61. https://doi.org/10.1016/j.ymben.2010.05.001.
[37] Palazzotto E, Tong Y, Lee SY, Weber T. Synthetic biology and metabolic engineering of actinomycetes for natural product discovery. Biotechnol Adv 2019;37:107366. https://doi.org/10.1016/j.biotechadv.2019.03.005.
[38] Blin K, Shaw S, Augustijn HE, Reitz ZL, Biermann F, Alanjary M, et al. antiSMASH 7.0: new and improved predictions for detection, regulation, chemical structures and visualisation. Nucleic Acids Res 2023;51:W46–50. https://doi.org/10.1093/nar/gkad344.
[39] Song X, Diao J, Yao J, Cui J, Sun T, Chen L, et al. Engineering a central carbon metabolism pathway to increase the intracellular Acetyl-CoA pool in *Synechocystis* sp. PCC 6803 grown under photomixotrophic conditions. ACS Synth Biol 2021;10:836–46. https://doi.org/10.1021/acssynbio.0c00629.
[40] Pang G, Sun T, Ding M, Li J, Zhao Z, Shen Q, et al. Characterization of an exceptional fungal mutant enables the discovery of the specific regulator of a silent PKS–NRPS hybrid biosynthetic pathway. J Agric Food Chem 2022;70:11769–81. https://doi.org/10.1021/acs.jafc.2c03550.
[41] Jiang K, Jin Y, Luo P, Wang X, Zhang Y, Shi T, et al. Exploration of the pneumocandin biosynthetic gene cluster based on efficient CRISPR/Cas9 gene editing strategy in *Glarea lozoyensis*. Int J Biol Macromol 2024;279:135220. https://doi.org/10.1016/j.ijbiomac.2024.135220.
[42] Li L, Zhao Y, Ruan L, Yang S, Ge M, Jiang W, et al. A stepwise increase in pristinamycin II biosynthesis by *Streptomyces pristinaespiralis* through combinatorial metabolic engineering. Metab Eng 2015;29:12–25. https://doi.org/10.1016/j.ymben.2015.02.001.
[43] Zhao X, Gao H, Wang Y, Wang Z, Zhou J. Efficient synthesis of phycocyanobilin by combinatorial metabolic engineering in *Escherichia coli*. ACS Synth Biol 2022;11:2089–97. https://doi.org/10.1021/acssynbio.2c00016.
[44] Men P, Zhou Y, Xie L, Zhang X, Zhang W, Huang X, et al. Improving the production of the micafungin precursor FR901379 in an industrial production strain. Microb Cell Factories 2023;22:44. https://doi.org/10.1186/s12934-023-02050-0.
[45] Lee JW, Na D, Park JM, Lee J, Choi S, Lee SY. Systems metabolic engineering of microorganisms for natural and non-natural chemicals. Nat Chem Biol 2012;8:536–46. https://doi.org/10.1038/nchembio.970.
[46] Park JH, Lee KH, Kim TY, Lee SY. Metabolic engineering of *Escherichia coli* for the production of L-valine based on transcriptome analysis and in silico gene knockout simulation. Proc Natl Acad Sci U S A 2007;104:7797–802. https://doi.org/10.1073/pnas.0702609104.
[47] Guo J, Sun X, Yuan Y, Chen Q, Ou Z, Deng Z, et al. Metabolic engineering of *Saccharomyces cerevisiae* for vitamin B5 production. J Agric Food Chem 2023;71:7408–17. https://doi.org/10.1021/acs.jafc.3c01082.
[48] Jin Z, Jin X, Jin Q. Conjugal transferring of resistance gene ptr for improvement of pristinamycin-producing *Streptomyces pristinaespiralis*. Appl Biochem Biotechnol 2010;160:1853–64. https://doi.org/10.1007/s12010-009-8691-z.
[49] Li H, Gao W, Cui Y, Pan Y, Liu G. Remarkable enhancement of bleomycin production through precise amplification of its biosynthetic gene cluster in *Streptomyces verticillus*. Sci China Life Sci 2022;65:1248–56. https://doi.org/10.1007/s11427-021-1998-8.